

## IN-SITU DAMAGE INVESTIGATION OF ADHESIVELY BONDED COMPOSITE REPAIRS

C. Hanneschläger<sup>1</sup>, F. Röper<sup>2</sup>, M. Wolfahrt<sup>2</sup>, G. Kucher<sup>3</sup>, B. Plank<sup>1</sup> and J. Kastner<sup>1</sup>

<sup>1</sup> University of Applied Sciences Upper Austria, Stelzhamerstrasse 23, 4600 Wels, Austria  
Email: christian.hanneschlaeger@fh-wels.at, bernhard.plank@fh-wels.at and  
johann.kastner@fh-wels.at, Web Page: <http://www.3dct.at/cms2/index.php/en/about-ctrq/team>

<sup>2</sup> Polymer Competence Center Leoben GmbH, Roseggerstraße 12, 8700 Leoben, Austria  
Email: florian.roeper@pccl.at and markus.wolfahrt@pccl.at

<sup>3</sup> FACC Operations GmbH, Breitenbach 52, 4973 St. Martin im Innkreis, Austria  
Email: g.kucher@facc.com

**Keywords:** x-ray tomography, in-situ, scarf repair, adhesive bonding, CFRP

### Abstract

In aeronautic industries adhesive bonding is a common technique to repair composites. In this study interrupted in-situ observations by X-ray computed tomography (XCT) were used to investigate the crack initiation and propagation in scarf repaired CFRP-laminates. Specimens were tested in two conditions: i) as-received ii) after conditioning under hot/wet conditions to determine the moisture influence on the damage behaviour. The specimens were tested in-situ in a high resolution XCT device with a voxel size of  $(8 \mu\text{m})^3$  at different load levels. The defects of each load step were segmented and compared to each other. An influence of the absorbed moisture neither on the damage propagation behaviour nor on the tensile strength could be observed. In particular, a concentration of cracks in the area of repair-ply terminations of the scarf joint could be determined.

### 1. Introduction

An increasing demand of cost-efficient and reliable repair methods for carbon fibre reinforced polymers (CFRP) can be observed due to the rising usage of CFRP laminates in primary aircraft structures [1]. Bonded scarf repair is a common technique in aeronautic industries for primary, secondary and tertiary aircraft structures. Several studies showed different methods for repairing CFRP. In our case we used the scarf repair technique due to its structural efficiency [2].

To understand the material behaviour under stress a microstructural investigation of the damage morphology is necessary. High resolution X-ray computed tomography (XCT) is a common non-destructive technique to characterise internal defects in CFRP specimens. The in-situ XCT method has already been used in several studies to investigate damage mechanisms in CFRP [3-6].

In this paper, the interrupted in-situ computed tomography technique was used to track the damage evolution of a scarf repaired CFRP-laminate. This method allows to visualize and quantify the damage volume at certain load levels. Therefore a determination of different damage types and their influence on the final failure is possible.

## 2. Experimental Method

### 2.1. Material and specimens

An epoxy resin based adhesive including a carrier was used in order to repair a parent-laminate with a soft patch repair approach (see Figure 1). The parent-as well as the repair-laminate consisted of an epoxy based, woven carbon fibre reinforced prepreg with a quasi-isotropic layup:  $[45/0/-45/90]_s$ . The parent-laminate and subsequently, during the repair process, the adhesive as well as the repair-plyes were cured in an autoclave following the cure parameters recommended by the manufacturers (180 °C, 2 h, 6.6 bar). Specimens were tested in two conditions: i) as-received ii) after conditioning under hot/wet conditions (70 °C / 85 % r. h.) for 8 weeks in order to determine the influence of moisture on the damage initiation and propagation. A reference-specimen was weighed before and after all in-situ investigations, to ensure a stable moisture content over all XCT scans.

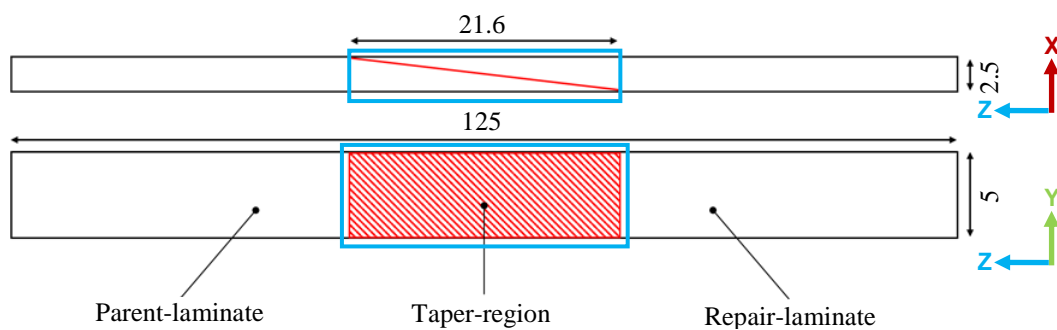


**Figure 1.** Schematic image of the repair-specimen (dimensions in mm; red: adhesive, blue: region of interest for XCT measurements).

### 2.2. High-resolution XCT

The scans with a voxel size of  $(8 \mu\text{m})^3$  were performed with a Nanotom 180NF XCT device (GE phoenix | X-ray). This system consists of a 180 kV sub- $\mu$ -focus X-ray tube and a 2304x2304 pixel flat panel pixel detector (Hamamatsu). Two scans were used to measure the whole height of the taper-region. As target material tungsten on a CVD window was used. The scan time per load level was 50 min. A beam hardening correction was applied to the data. The 3D volume was analysed by using the software VGStudio MAX 3.1.

### 2.2. In-situ tensile stage

In-situ observation was done using a CT5000 5 kN in-situ tensile stage (Deben) at room temperature. An interrupted tensile-test was used to detect damage at several load stages. The load rate was set to 1 mm/min. Reference-specimens with the same geometry as depicted in figure 1 were tested ex situ to define the maximum Force  $F_{\text{max}}$  as well the load steps of both specimen conditions. Table 1 shows the planned load steps and the corresponding relative forces of the reference-specimens.

**Table 1.** Planned load steps for in-situ CT measurements.

Relative percentage of reference $F_{max}$ [%]	Failure [-]	As-received: Force [N]	Conditioned: Force [N]
0	-	0	0
85	-	3000	3000
95	-	3300	3400
~100	yes	3500	3600

## 2.4. Segmentation

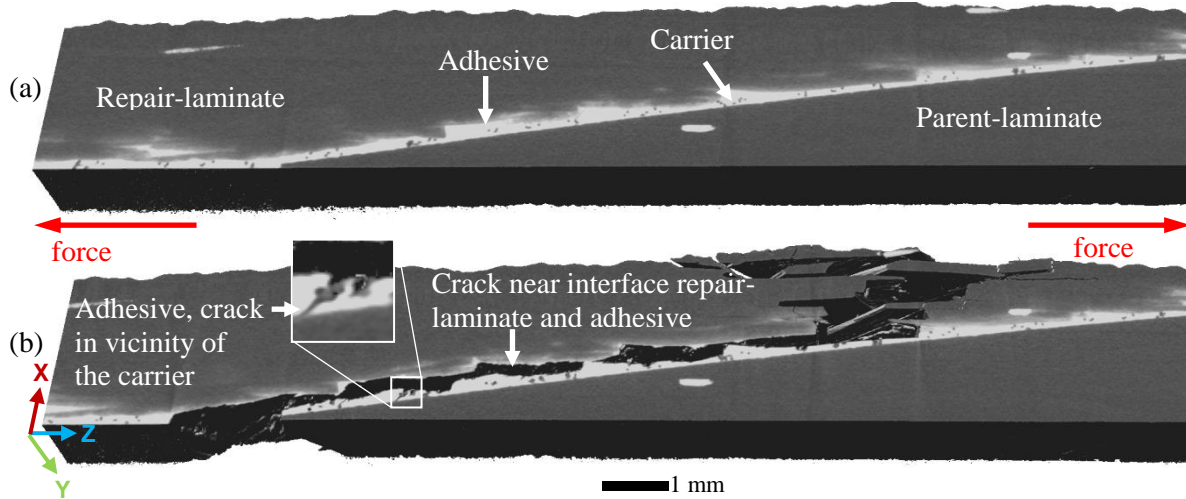
A manual mapping of the 32 bit XCT dataset to 16 bit was done, to ensure that the average grey peak level of the air (10,000) and the adhesive (50,000) is constant for all individual scans. A non-local means filter (smoothing value 1.5) was applied to preserve the edges of the cracks during noise reduction. An additional subtracting gauss (3x3x3) filter was used to improve the contrast between cracks and the specimen material. To eliminate the influence of the surrounding air the surface determination of VGStudio MAX 3.1 (ISO-50 threshold) was used. The surface near region was excluded from the evaluation, due to artefacts (for example beam hardening). The defect segmentation was applied on the differential volume (non-local means subtracting gauss filtered) of the resulting region of interest. Pore segmentation was achieved by the VGStudio pore analysis tool, the threshold from (Eq. 1) was used.  $\mu$  is defined as the mean grey value of the peaks.  $\sigma$  is the standard deviation.

$$threshold = \mu_{materialpeak} - 4 \sigma_{materialpeak} \quad (1)$$

To separate defects from noise the minimum defect size was defined as 14 voxel. Defects with a sphericity value bigger than 0.7 were sorted out as false positive defects. This segmentation threshold and method was determined empirically.

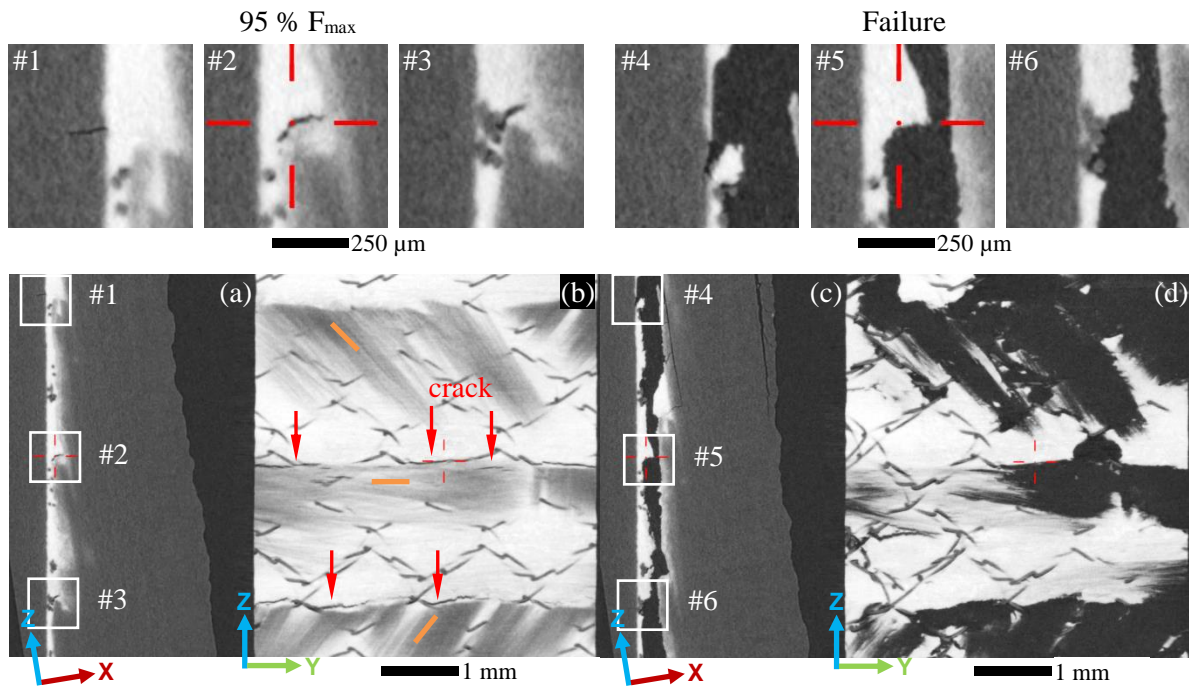
## 4. Results and discussion

Comparison of the increasing damage sizes between the individual load levels allows to monitor crack initiation and progression. Initial cracks can be observed at the first load step (85 % of reference  $F_{max}$ ). An increase in damage size can be determined at 95 % of the reference's  $F_{max}$ . Figure 2 shows a 3D comparison of the unloaded and broken state of the as-received specimen. Adhesive, carrier and CFRP matrix can be detected, but the contrast is too low to identify the individual rovings. Nevertheless a final fracture in the vicinity of the interface between the adhesive and the repair-laminate can be determined. In the mid-section of the specimen (with respect to the z-axis) cracks also grow through the plies of the repair-laminate in x-direction until the surface is reached. Smaller cracks between carrier and adhesive are also visible and are highlighted.



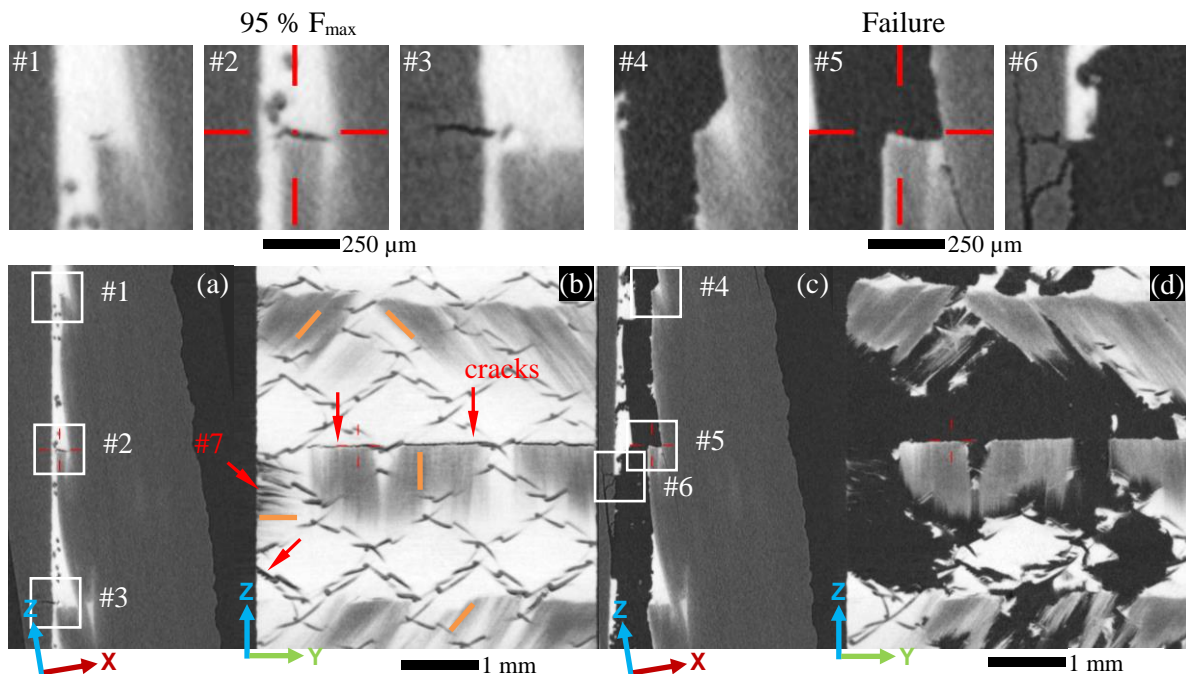
**Figure 2.** Condition as-received: 3D comparison of the unloaded (a) and the broken (b) specimen.

Figure 3 shows a comparison of the as-received specimen directly before (95 %  $F_{max}$ ) and after failure. An influence of the ply orientation on the crack origin and propagation cannot be seen (see figure 3 (b)). The damage types identified are: cracks in the parent-laminate (see figure 3 detail 1), interface cracks between repair-laminate and adhesive (see figure 3 detail 2) and interface cracks between carrier and adhesive (see figure 3 detail 3). It is obvious that the cracks between the repair-laminate and the adhesive as well as in the parent-laminate are expanding in y-direction (z-direction = load direction) in the vicinity of the repair-ply-terminations of the scarf joint. The crack in the parent-laminate (transverse direction, see figure 3 detail 1) is closed after the specimen's failure (see figure 3 detail 4). Cracks in the repair-laminate (longitudinal direction) are visible in the broken specimen.



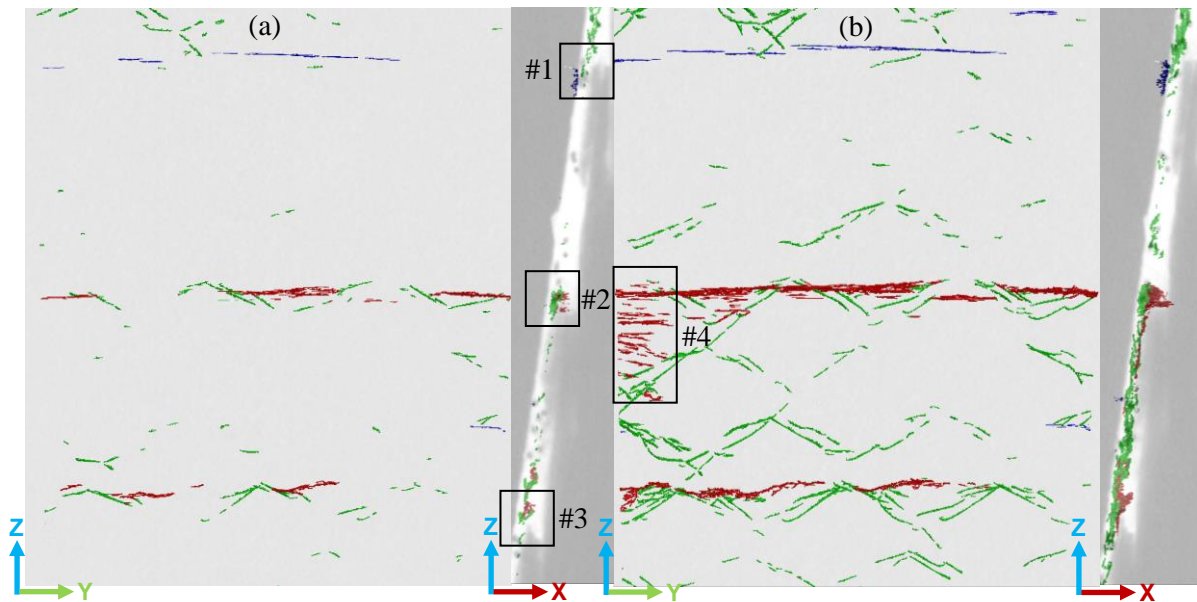
**Figure 3.** Comparison of load step 95 %  $F_{max}$  and failed state of as-received specimen (slice images): (b) and (d) ply orientation (highlighted orange where applicable) close to the adhesive, (a) and (c) overview bondline, laminate and (1)-(6) respective details.

Figure 4 shows a comparison of the conditioned specimen directly before (95 %  $F_{max}$ ) and after failure. A mass loss (moisture) of 0.09 % was detected during in-situ investigation. Regarding the maximum force at failure, no significant influence of the conditioning could be investigated. In general, the same damage types as for the as-received specimen can be observed, which are propagating in the same direction as in the as-received specimen. Transversal and longitudinal cracks in the parent-laminate after failure are shown in figure 4 detail 6. Furthermore cracks in the repair-adhesive in the y-z-plane oriented from the specimen boarder to the centre are visible (see figure 4 detail 7).



**Figure 4.** Comparison of load step 95 %  $F_{max}$  and failed state of conditioned specimen (slice images): (b) and (d) ply orientation (highlighted orange where applicable) close to the adhesive, (a) and (c) overview bondline, laminate and (1)-(7) respective details.

Figure 5 shows the segmented damage propagation of the as-received specimen. The defects are colour-coded according to their type. In load stage 85 %  $F_{max}$  first cracks can be detected mainly in the vicinity of the terminations of the repair-ply (see figure 5 detail 1 - 3). Mollenhauer et al. mentioned a strain concentration induced by changes of the adhesive thickness (resin rich pockets) of adhesively repaired CFRP [7]. The strain concentration in the areas with higher adhesive thickness as main factor for the initiation of cracks is plausible in this case. Furthermore no significant influence of the ply-orientation on the formation of cracks could be detected. It can be observed that the cracks in the vicinity of the interface between the adhesive and the repair-ply as well as in the parent-laminate are growing in y-direction along the terminations of the repair-ply (see figure 5 (b)). This behaviour is expected due to the fact that the load-direction is perpendicular to the x-y-plane. In comparison to this the cracks between carrier and adhesive are expanding along the respective interface.



**Figure 5.** Comparison of segmented defects at different load steps ((a): 85 %  $F_{max}$ ; (b): 95 %  $F_{max}$ ) for the as-received specimen. Defects are colour-coded by type (green: interface cracks between adhesive and carrier; red: cracks in the vicinity of the interface between adhesive and repair-laminate; blue: cracks in parent-laminate).

#### 4. Conclusions

It has been shown that the interrupted in-situ investigations by XCT techniques are a suitable method for tracking the damage propagation of adhesively bonded composite repairs during a tensile test. The results of the as-received specimen were compared to a conditioned specimen. A voxel size of  $(8 \mu\text{m})^3$  was applied for the detection of cracks at the two load steps (85 and 95 % of  $F_{max}$ ). An influence of the moisture content on the crack initiation and propagation behaviour could not be seen. The detected and segmented failure types are cracks between carrier and adhesive, cracks in the vicinity of the interface between repair-laminate and adhesive as well as cracks in the parent-laminate (longitudinal and transverse direction). It has been confirmed that the ply orientation of the adhesive nearest ply has no significant effect on the crack initiation and propagation. The damage initiation occurs in the regions of the repair-ply terminations (areas of variations in adhesive thickness) of the scarf joint. It can be assumed that the strain concentration at these adhesive-rich areas is causing the first defects. In the next load step the cracks are growing mainly in y-direction along the scarf edge (plane x-y). Further work will be carried out in order to determine the influence of moisture on saturated specimens at a test temperature of 70 °C. In this context, Ahn et al. [8] showed a decrease of tensile strength for repaired laminates at comparable conditions.

#### Acknowledgments

The research work was performed at the University of Applied Sciences Upper Austria and the Polymer Competence Center Leoben GmbH (PCCL, Austria) within the framework of the COMET-program of the Federal Ministry of Science, Research and Economy with contributions by the FACC Operations GmbH (Austria). The PCCL is funded by the Austrian Government and the State Governments of Styria, Lower Austria and Upper Austria. This work was additionally supported by the K-Project for “non-destructive testing and tomography plus” (ZPT+) and by the project “multimodal and in-situ characterization of inhomogeneous materials” (MiCi) and by the European Regional Development Fund (EFRE) in the framework of the EU-program IWB2020.

## References

- [1] K. B. Katnam, L. F. M. Da Silva and T. M. Young. Bonded repair of composite aircraft structures: a review of scientific challenges and opportunities, *Prog. Aerosp. Sci.*, 61:26–42, 2013.
- [2] S. B. Kumar, I. Sridhar, S. Sivashankera, S. O. Osiyemib and A. Bag. Tensile failure of adhesively bonded CFRP composite scarf joints, *Materials Science and Engineering: B.*, 132:113–120, 2006.
- [3] A. Amirkhanov, A. Amirkhanov, D. Salaberger, J. Kastner, M. E. Gröller and C. Heinzl. Visual analysis of defects in glass fiber reinforced polymers for 4DCT interrupted in situ tests, *Computer Graphics Forum*, 35:201-210, 2016.
- [4] S. Senck, D. Salaberger, C. Gusenbauer, B. Plank, G. Rao and J. Kastner. Talbot-Lau grating interferometer XCT for the quantitative characterization of damage in polymers after impact and static tensile testing, *Proceeding 19th World Conference on Non-Destructive Testing WCNDT2016, Munich, Germany*, June 13-17 2016.
- [5] D. J. Bull, S. M. Spearing and I. Sinclair, Observations of damage development from compression-after-impact experiments using ex situ micro-focus computed tomography, *Composites Science and Technology*, 97:106-114, 2014.
- [6] M. G. R. Sause. *In Situ Monitoring of Fiber-Reinforced Composites*. Springer Series in Material Science, 2016.
- [7] D. H. Mollenhauer, B. M. Fredrickson, G. A. Schoeppner, E. V. Iarve and A. N. Palazotto. Moiré interferometry measurements of composite laminate repair behavior: Influence of grating thickness on interlaminar response, *Composites: Part A*, 39:1322-1330, 2008.
- [8] S. H. Ahn and G. S. Springer. Repair of Composite Laminates, *Technical Report*, 2000.